A Preliminary Animal Experiment to Assess the Efficacy of a Novel Non-Osteotomy Implant for the Correction of the Angular Deformity and Limb Length Discrepancy

Taegyun Roh *

Posted Date: 23 March 2026

doi: 10.20944/preprints202603.1757.v1

Keywords: growth and development; growth plate; femur; animal experimentation; tensile strength

 doi:10.20944/preprints202603.1757.v1

Article

A Preliminary Animal Experiment to Assess the Efficacy of a Novel Non-Osteotomy Implant for the Correction of the Angular Deformity and Limb Length Discrepancy

Taegyun Roh

Department of Orthopaedic Surgery, Bundang Jesaeng General Hospital, Seongnam, Gyeonggi 13590, Republic of Korea; rohtaegyun@gmail.com.

Abstract

Background: A new-concept of non-osteotomy implant is advantageous in *not only* performing a surgery by applying the tensile force to the growth plate without osteotomy *but also* achieving a prompt recovery; it is expected to be effective in correcting the leg length discrepancy and angular deformity. **Objectives:** This animal experiment was performed to assess the effectiveness of a new-concept of non-osteotomy implant in correcting the leg length discrepancy and angular deformity by promoting the growth without suppressing it. **Methods:** To compare differences in changes in anthropometric measurements between preoperatively and postoperatively, the right and left sides of the femur served as the experimental group and the control group, respectively. In the right femur, two screws each were placed in the upper and lower part of the growth plate. For bilateral distraction, a spring was applied to both sides of the femur (experimental animals 9 and 10). For unilateral distraction, a spring was applied to the external side of the femur only (experimental animals 5, 7, 8 and 11). A CT was performed at a 4-week interval and CT scans were reconstructed 3-dimensionally the Mimics® Innovation Suite (Mimics and 3-matic; Materialize, Leuven, Belgium). The anatomical axis of the femur (AAF) is considered as a line that passes through the long axis of the femur through the medullary canal. The mechanical axis of the femur (MAF) is the line drawn through the centers of the femoral head and the intercondylar fossa. This was followed by measurement of time-dependent changes in the line and angle formed by the AAF and the MAF. In more detail, a 3-D registration was performed for CT scans of the femur at each time point, for which the lower part of the growth plate was matched and both the AAF and the MAF were used to form the plane. This was followed by 3-D orthogonal projection of both the AAF and the MAF on the plane postoperatively. **Results:** With bilateral distraction at a tensile force of 50 N and 100 N, the degree of changes in the length of the AAF at 1 month from baseline was higher on the right side as compared with the left side. This was also seen in the length of the MAF. Moreover, with unilateral distraction at a tensile force of 25 N and 50 N, the degree of changes in the angle formed by the AAF at 1, 2, 3, 4, 5 and 6 months from baseline was significantly higher on the right side as compared with the left side ($P<0.05$). This was also seen in the angle formed by the MAF. **Conclusions:** The current results confirm the biomechanical effectiveness of a new-concept of non-osteotomy implant in promoting the bone growth. But this deserves further prospective randomized controlled trials.

Keywords: growth and development; growth plate; femur; animal experimentation; tensile strength

1. Introduction

In humans, physical development is a process that is continued since childhood. It is characterized by changes in the body size and appearance as well as the development of secondary sexual characteristics [1]. Children tend to have body shapes and sizes similar to their parents or

 doi:10.20944/preprints202603.1757.v1

grandparents, although other factors, such as nutrition, genetic predisposition and maternal-fetal health, may have a considerable effect on their growth [2–4].

Childhood is characterized by the maturation of the growth plate (GP). This is followed by a decrease in its total width and disappearance of it at the end of puberty. Then, the GP is completely replaced with bone and the longitudinal growth is finished accordingly [5,6].

Also known as the physis, the GP is the cartilaginous portion at the ends of long bones. It is characterized by high metabolic activity and is regulated by diverse types of hormones and signaling pathways. But this may be impaired by trauma, medications and other extrinsic factors, which may eventually lead to the GP abnormalities and subsequent growth disturbances [7].

Internal fixatives that are currently used for asymmetrical physeal suppression include staples, transphyseal screw and an 8-plate implant, which are representative of a tension band plate, and Ilizarov external fixatives [8,9]. Nevertheless, the occurrence of complications due to internal fixatives poses a challenge for orthopedic surgeons. That is, use of staples may cause such complications as pain, joint swelling, irritation during joint motion, superficial infection, a delay in the recovery of range of motion and hypercorrection or hypocorrection of the leg alignment. Moreover, use of transphyseal screw may cause irreversible cessation of growth. In addition, there may be a delay in the appearance of the inhibitory effects against the GP. Because the rate of suppression does not reach 100%, there may be cases of hypocorrection. Complications of an 8-plate implant include a possible risk of suppression of the growth of the contralateral GP if a screw crosses the center of the GP although it can be theoretically postulated that use of a long screw may increase the length of moment arm and thereby raise the force of compression. Finally, complications of external fixatives include a decrease in the patient convenience and a risk of growth impairment due to the fracture of the GP [10,11].

Currently, external fixatives are frequently used to correct the deformity by causing damages to the GP or diaphysis. Use of external fixatives is an effective modality, although its disadvantages include a high cost, patient inconvenience and relatively greater risks of complications, such as patient inconvenience, non-union, joint pain and stiffness of the ligament. It is therefore imperative that a novel technology be developed as an alternative to an external fixative [12–15]. This justifies the development of a new concept of non-osteotomy implant that is characterized by application of the distraction force to the GP after an in vivo placement for the purposes of increasing the potential growth. Its advantages include convenient surgery and prompt recovery performing; its indications may include leg length discrepancy (LLD) and angular deformity (AD). It is therefore expected to overcome demerits of currently available surgical options for suppression of the GP.

Given the above background, we conducted this animal experiment to assess the efficacy and safety of a new concept of non-osteotomy implant assess in correcting the LLD and AD by promoting the growth without suppressing it.

2. Materials and Methods

2.1. Experimental Design and Setting

To determine the appropriate size of both the growth plate and an implant, anatomical structures of the ilium of normal experimental animals were analyzed using X-ray and computed tomography (CT) scans. This is *not only* because the site of implantation should be available at a length of approximately 2.5 cm on X-ray images *but also* because the tibia is not sufficient for the implantation. Therefore, the femur was determined to be the site of implantation. The location of the growth plate was determined, and the post-implantation course was monitored under homogeneous conditions. To do this, CT scans were taken to perform an accurate, meticulous monitoring of the post-implantation course because their advantages include higher resolution and easier-to-use as compared with X-ray images. But there is a possibility that a CT may cause an artifact depending on the characteristics of an implant.

 doi:10.20944/preprints202603.1757.v1

2.2. Biomechanical Test

A biomechanical study was performed to determine the breaking load of the growth plate. To determine the breaking load of the distal growth plate of the posterior femur of a 12-month-old Beagle, the tensile strength was applied to it using the MTS 858 Bionix (MTS Systems, Eden Prairie, MN, USA). Therefore, the distal part of the posterior femur served as the sample for the biomechanical test.

2.3. Preparation of the Experimental Sample

After the removal of the soft tissue, such as the muscle or ligament, the location of the growth plate was confirmed on X-ray and CT scans. This was followed by the fixation of the distal femur involving the growth plate using a dental resin (Vertex Trayplast green). Meanwhile, special attention should be paid to the possibility that the cartilage might lower the adhesion property of the resin. A screw should therefore be used for the fixation in a similar manner to the actual surgical procedure.

2.4. A Breaking Test for the Growth Plate

The sample was fixed to the MTS 858 Bionix (MTS Systems) and then given the tensile strength in a displacement controlled mode at a rate of 0.004 mm/s.

2.5. Design of an Implant and Preparation of the Sample

Fixed load data was collected for the development of an implant. To apply a fixed load to an implant, an orthopedic bone screw was designed. Considering that the bone screw cannot be removed from the human body when there is an erosion on the inner socket while a conventional type of orthopedic bone screw is loosened, however, the head of a screw was modified from a round to a hexagonal shape. This made it possible to loosen an orthopedic bone screw despite the erosion on the inner socket. Moreover, an orthopedic bone screw was also designed in such a manner that self-tapping could be performed without additional tapping. Furthermore, a reverse cutting flute was designed on the thread of a screw in the proximal area to the shaft with reference to a catalogue of a benchmarked product. Thus, attempts were made it easier to pull out a screw while it is loosened.

2.6. Preparation of and Revision to the Primary Sample of an Implant

A shape-memory alloy spring and the inner structure supporting its alignment for bone growth were designed. This was followed by the preparation of the primary sample of an implant using 3-dimensional (3-D) printer to assess both a fixed load and a tensile load in accordance with the ASTM F543: Standard Specification and Test Methods for Metallic Medical Bone Screws by outsourcing to the Implanova by Dental Evolutions Inc. (Beverly Hills, CA). A screw was horizontally inserted in the ilium for the application of fixed load to the sample. To do this, a guide pin should be inserted in the target area using a guide. Then, the depth of insertion was measured using a gauge and a desired amount of space was confirmed before the insertion of a screw.

2.7. Assessment of the Performance of an Implant

The sample was fixed to the MTS 858 Bionix (MTS Systems) and its axial pull-out strength, torsion strength and bending strength were measured after being given a tensile load, a torsion load and a bending load were measured at a rate of 5 mm/s, 1 r/min and 5 mm/s, respectively, in a displacement controlled mode.

 doi:10.20944/preprints202603.1757.v1

2.8. A Preliminary Assessment of Biological Safety of Spring

Biological safety of spring was assessed according to the International Organization for Standards (ISO) 10993 - Biological Evaluation of Medical Devices, as summarized in Table 1.

Table 1. International Organization for Standards (ISO) 10993 - Biological Evaluation of Medical Devices.

ISO No.	Year of latest update	Details
ISO 10993-1	2009	Evaluation and testing in the risk management process
ISO 10993-3	2003	Tests for genotoxicity, carcinogenicity and reproductive toxicity
ISO 10993-4	2002/ Amd 1:2006	Selection of tests for interactions with blood
ISO 10993-5	2009	Tests for in vitro cytotoxicity
ISO 10993-6	2007	Tests for local effects after implantation
ISO 10993-7	2008	Ethylene oxide sterilization residuals
ISO 10993-8	2001	Selection of reference materials
ISO 10993-9	1999	Framework for identification and quantification of potential degradation products
ISO 10993-10	2010	Tests for irritation and delayed-type hypersensitivity
ISO 10993-11	2006	Tests for systemic toxicity
ISO 10993-12	2012	Sample preparation and reference materials
ISO 10993-14	2001	Identification and quantification of degradation products from ceramics
ISO 10993-16	1997	Toxicokinetic study design for degradation products and leachables
ISO 10993-17	2002	Establishment of allowable limits for leachable substances
ISO 10993-18	2005	Chemical characterization of materials
ISO/ TS 10993-19	2006	Physico-chemical, morphological and topographical characterization of materials
ISO/ TS 10993-20	2006	Principles and methods for immunotoxicology testing of medical devices

2.8.1. MTT Assay

The MTT assay was performed to assess the cell viability. The yellow dye 3(4,5-dimethylthiazol-2-yl)-2,5-diphenyl tetrazolium bromide (MTT) is reduced by mitochondrial dehydrogenase in living cells to produce insoluble purple MTT formazan crystals which, after solubilization, can be measured spectrophotometrically. This property has long been used to assess the viability of cells [16]. In this experiment, murine fibroblasts (L-929; Korean Cell Line Bank, Seoul, Korea) were cultured for a certain period of time and then treated with MTT dissolved in phosphate buffered saline. This was followed by culture of murine fibroblasts at 37°C for a certain period of time. After a complete removal of the media containing MTT, purple-colored formazan crystals formed in viable cells were dissolved using dimethyl sulfoxide (DMSO). Then, the optical density (OD) was measured using an enzyme-linked immunosorbent assay (ELISA) reader at a wavelength of 450 nm. To do this, murine fibroblasts were directly treated with the elution, followed by the assessment of its effects on the growth, death or other phenomena of viable cells. The OD was measured in triplicate and then averaged.

 doi:10.20944/preprints202603.1757.v1

2.8.2. Acute Systemic Toxicity Test

The elution (50 mL/kg) and the blank reagent solution (50 mL/kg) were injected in the tail vein and the abdominal cavity of mice at a rate of 100 μL/s in the trial group and the control group, respectively. At certain time points (4, 24, 48 and 72 hr), changes in common clinical symptoms were monitored. In all the experimental animals, the body weight and the number of deaths were compared between before and after the treatment (Table 2).

Table 2. Preparation of the sample solution and test system.

Negative control: 0.9% sterilized saline cotton seed oil	Experimental animal: ICR mouse
	Sex: Male
Elution solvent: 0.9% sterilized saline cotton seed oil	Age: 5 weeks
Ratio of elution: 4 g/20 mL, Temperature/time of elution: 37±2°C / 72±2 hr	

2.8.3. Sensitization Test

A sensitization test was performed using a young, healthy guinea pig weighing 300 g. In the intradermal induction phase, experimental animals were intradermally given a symmetric injection of three solutions using a 26-G needle-attached syringe at a respective volume of 0.1 mL on both sides of the back. Solution 1 is a mixture of a saline and Freund's complete adjuvant at the same volume fraction. Solution 2 is an elution in the trial group and a saline in the control group. Solution 3 is a mixture of solution 1 and 2 at the same volume fraction.

One week later, the patch (20 mm × 40 mm) was applied to the site of intradermal injection. At 48 h after dressing, it was removed. Two weeks thereafter, the hair was shaved on either side of the flank. Then, the patch (10 mm × 10 mm) was applied to the site of intradermal injection. At 24 h after dressing, it was removed. Time-dependent changes in the findings seen at 24 and 48 h were monitored. Thus, the degree of sensitization was assessed based on the Magnusson and Kligman scale, as previously described [17].

2.9. Assessment of the Efficacy

To compare differences in changes in anthropometric measurements between preoperatively and postoperatively, the right and left sides of the femur served as the experimental group and the control group, respectively. In the right femur, two screws each were placed in the upper and lower part of the growth plate. For bilateral distraction, a spring was applied to both sides of the femur (experimental animals 9 and 10). For unilateral distraction, a spring was applied to the external side of the femur only (experimental animals 5, 7, 8 and 11). A CT was performed at a 4-week interval and CT scans were reconstructed 3-dimensionally the Mimics® Innovation Suite (Mimics and 3-matic; Materialize, Leuven, Belgium).

The anatomical axis of the femur (AAF) is considered as a line that passes through the long axis of the femur through the medullary canal [18]. The mechanical axis of the femur (MAF) is the line drawn through the centers of the femoral head and the intercondylar fossa [19]. This was followed by measurement of time-dependent changes in the line and angle formed by the AAF and the MAF.

In more detail, a 3-D registration was performed for CT scans of the femur at each time point, for which the lower part of the growth plate was matched and both the AAF and the MAF were used to form the plane. This was followed by 3-D orthogonal projection of both the AAF and the MAF on the plane postoperatively.

 doi:10.20944/preprints202603.1757.v1

2.10. Statistical Analysis of the Experimental Data

All data was expressed as mean±standard deviation or the number of the experimental animals with percentage, where appropriate. First, we analyzed whether there were any differences in time-dependent changes in the length of the AAF or the MAF from baseline between the right and left sides of the femur. Second, we also analyzed whether there were any significant differences in time-dependent changes in the angle formed by the AAF or the MAF from baseline using Mann-Whitney U test. All statistical analyses were performed using the SPSS version 26 (SPSS Inc., Chicago, IL, USA). A P-value of <0.05 was considered statistically significant.

3. Results

3.1. A breaking Test for the Growth Plate

The maximum loads applied to each sample are summarized in Table 3, whose mean values are calculated as 754.33±66.88 N. Based on these results and considering that a maximum loads of 200 N is required to distract the growth plate, there might be no break in the growth plate.

Table 3. Maximum loads applied to each sample.

Sample	Maximum loads (N)
1	650.45
2	830.75
3	755.53
4	783.68
5	821.11
6	684.44
7	Non-applicable
8	Non-applicable

3.2. Acute Systemic Toxicity Test

Throughout the experiment, there were no deaths or notable clinical symptoms in all the groups (Table 4).

Table 4. Clinical symptoms.

Eluate	Time points of observation									
	Immediately after administration		4 hr		24 hr		48 hr		72 hr	
	T	C	T	C	T	C	T	C	T	C
SC	AN	AN	AN	AN	AN	AN	AN	AN	AN	AN
CSO	AN	AN	AN	AN	AN	AN	AN	AN	AN	AN

Note: T, trial group; C, control group; AN, normal.

In the polar negative control group, the body weight of experimental animals at 0 and 24 days was measured as 323.72±20.84 g and 446.94±26.45 g, respectively. In the non-polar negative control group, these measurements were 319.84±17.32 g and 460.30±27.05 g in the corresponding order. Moreover, there were no experimental animals showing ≥10% decrease in the body weight at 3 days from 0 day (Tables 5 and 6). Furthermore, autopsy of survived experimental animals revealed no notable gross findings in association with the administration of test substance.

 doi:10.20944/preprints202603.1757.v1

Table 5. The number of deaths and the body weight (Extract: 0.9% sterilized saline / cotton seed oil).

Route, dose and test substance	Control group				Trial group			
	Animal No.	Body weight (g)		Death / test	Animal No.	Body weight (g)		Death / test
		0 day	3 days			0 day	3 days	
I.V. 50 mg/kg (Polar eluate)	01	31.35	32.15	0 / 5	06	31.42	32.06	0 / 5
	02	29.54	30.91		07	29.09	30.93	
	03	30.15	30.99		08	29.42	29.91	
	04	29.89	30.49		09	29.23	30.21	
	05	29.30	29.87		10	29.58	30.79	
I.P. 50 mg/kg (Non-polar eluate)	11	30.84	31.94	0 / 5	16	30.15	32.12	0 / 5
	12	30.98	31.71		17	30.74	31.15	
	13	29.50	30.45		18	30.19	32.10	
	14	30.00	30.51		19	28.75	32.00	
	15	28.42	28.88		20	27.22	29.42	

Abbreviations: I.V., intravenous injection; I.P., intraperitoneal injection.

Table 6. Changes in the body weight and clinical symptoms (polar solvent: 0.9% sterilized saline / non-polar solvent: cotton seed oil).

Group	Animal No.	Sex	Body weight (g)		Changes in the body weight	Signs of toxicity[1]
			0 day	24 days		
Polar negative control group	N1	Female	353.11	444.54	91.43	None
	N2		334.16	405.98	71.82	
	N3		322.75	456.90	134.15	
	N4		306.44	448.54	142.10	
	N5		302.16	478.76	176.60	
Non-polar negative control group	N6	Female	342.90	455.65	112.75	None
	N7		327.88	496.55	168.67	
	N8		319.69	472.84	153.15	
	N9		305.71	423.08	117.37	
	N10		300.52	453.39	152.87	

[1]Summary of clinical observations – Day 0 through Day 23.

3.3. Differences in Time-Dependent Changes in the Length of and the Angle Formed by the AAF or the MAF from Baseline Between the Right and Left Sides of the Femur

With bilateral distraction at a tensile force of 50 N and 100 N, the degree of changes in the the length of the AAF at 1 month from baseline was higher on the right side as compared with the left side. This was also seen in the length of the MAF (Tables 7 and 8) (Figures 1 and 2).

Table 7. Time-dependent changes in the length of the anatomical axis of the femur from baseline.

Mode of distraction	Force	Time period	N	Values	
				ΔAAF	
				R	L
Bilateral	50 N	1 month - baseline	1	1.4	1.3
	100 N	1 month - baseline	1	1.76	0.88

Note: N, the number of the samples; ΔAAF, time-dependent changes in the length of the anatomical axis of the femur from baseline; R, right side; L, left side.

 doi:10.20944/preprints202603.1757.v1

Table 8. Time-dependent changes in the length of the mechanical axis of the femur from baseline.

Mode of distraction	Force	Time period	N	Values	
				ΔMAF	
				R	L
Bilateral	50 N	1 month - baseline	1	1.95	1.31
	100 N	1 month - baseline	1	3.00	1.55

Note: N, the number of the samples; ΔMAF, time-dependent changes in the length of the mechanical axis of the femur from baseline; R, right side; L, left side.

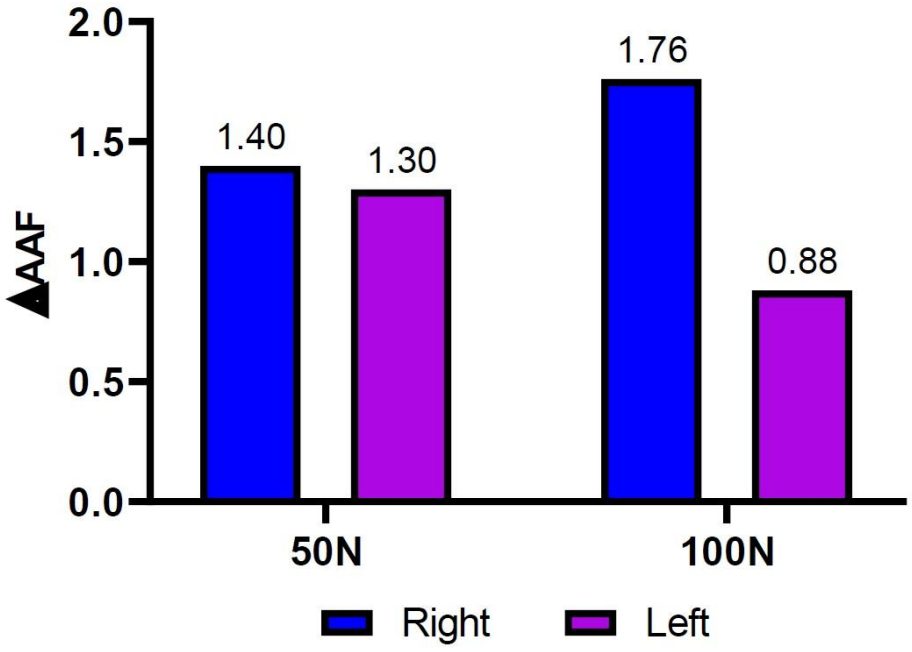

Figure 1. Changes in the anatomical axis of the femur after bilateral distraction at a force of 50 and 100 N.

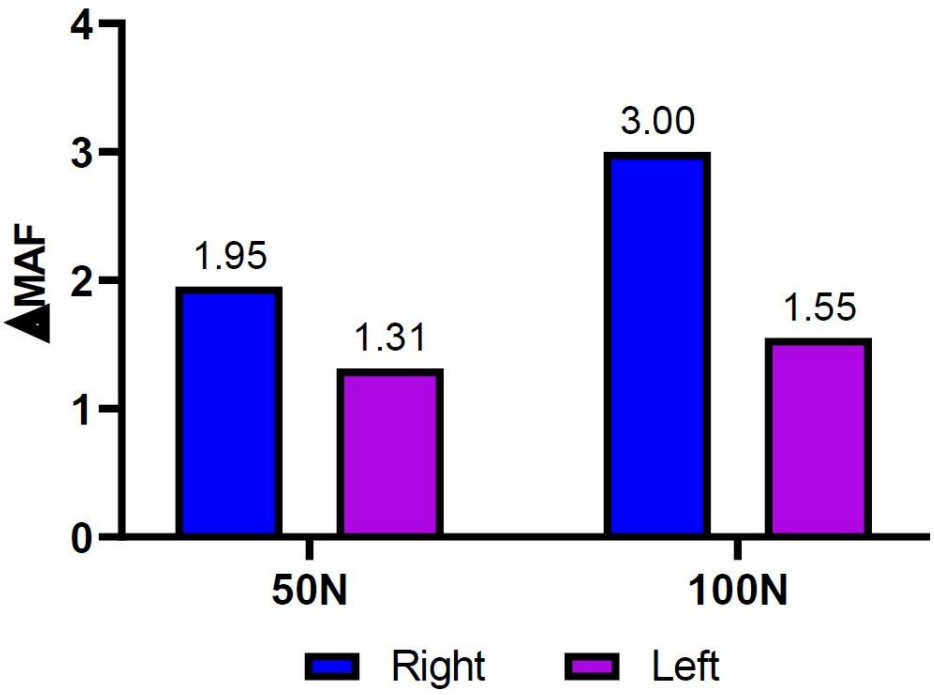

Figure 2. Changes in the mechanical axis of the femur after bilateral distraction at a force of 50 and 100 N.

 doi:10.20944/preprints202603.1757.v1

Moreover, with unilateral distraction at a tensile force of 25 N and 50 N, the degree of changes in the angle formed by the AAF at 1, 2, 3, 4, 5 and 6 months from baseline was significantly higher on the right side as compared with the left side (P<0.05). This was also seen in the angle formed by the MAF (Tables 9 and 10) (Figures 3 and 4).

Table 9. Time-dependent changes in the angle formed by the anatomical axis of the femur from baseline.

Mode of distraction	Force	Time points	Values ΔAAF		Z	P-value
			R	L		
Unilateral	25 N	Baseline	0.00±0.00	0.00±0.00	0.000	1.000
		1 month	0.56±0.11	-0.31±0.44	-2.289	0.039*
		2 months	1.44±0.11	-0.04±0.51	-2.363	0.024*
		3 months	2.60±0.87	-0.68±1.36	-2.365	0.024*
		4 months	3.62±1.12	-0.36±0.90	-2.419	0.020*
		5 months	4.30±1.42	-0.28±0.23	-2.715	0.008*
		6 months	4.96±1.82	-0.29±0.54	-3.247	0.001*
	50 N	Baseline	0.00±0.00	0.00±0.00	0.000	1.000*
		1 month	2.06±0.93	-1.22±1.27	-2.228	0.033*
		2 months	3.56±1.86	-0.61±0.71	-2.302	0.028*
		3 months	5.61±0.64	-0.41±1.61	-2.594	0.017*
		4 months	7.67±0.47	0.12±1.46	-2.735	0.008*
		5 months	10.24±0.03	-0.47±1.25	-3.115	0.002*
		6 months	12.47±0.33	0.16±0.74	-3.235	0.001*

Note: N, the number of the samples; ΔAAF, time-dependent changes in the angle formed by the anatomical axis of the femur from baseline; R, right side; L, left side. Values are mean±standard deviation. *Statistical significance at P<0.05.

Table 10. Time-dependent changes in the angle formed by the mechanical axis of the femur from baseline.

Mode of distraction	Force	Time points	Values ΔMAF		Z	P-value
			R	L		
Unilateral	25 N	Baseline	0.00±0.00	0.00±0.00	0.000	1.000
		1 month	0.98±0.36	0.28±0.51	-2.154	0.039*
		2 months	1.87±0.52	0.21±0.15	-2.204	0.033*
		3 months	3.00±0.97	-0.30±0.83	-2.362	0.024*
		4 months	3.90±1.17	0.00±0.17	-2.544	0.014*
		5 months	4.48±1.41	-0.22±0.08	-2.715	0.008*
		6 months	5.02±2.30	0.16±0.17	-3.266	0.001*
	50 N	Baseline	0.00±0.00	0.00±0.00	0.000	1.000*
		1 month	1.83±1.27	-2.12±2.11	-2.167	0.033*
		2 months	3.43±2.38	-1.63±1.42	-2.465	0.014*
		3 months	5.36±1.15	-1.40±2.02	-2.568	0.014*
		4 months	7.67±0.47	0.12±1.46	-2.898	0.005*
		5 months	10.24±0.03	-0.47±1.25	-3.083	0.005*
		6 months	12.47±0.33	0.16±0.74	-3.954	0.000*

Note: N, the number of the samples; ΔMAF, time-dependent changes in the angle formed by the mechanical axis of the femur from baseline; R, right side; L, left side. Values are mean±standard deviation. *Statistical significance at P<0.05.

(**a**) 25 N

 doi:10.20944/preprints202603.1757.v1

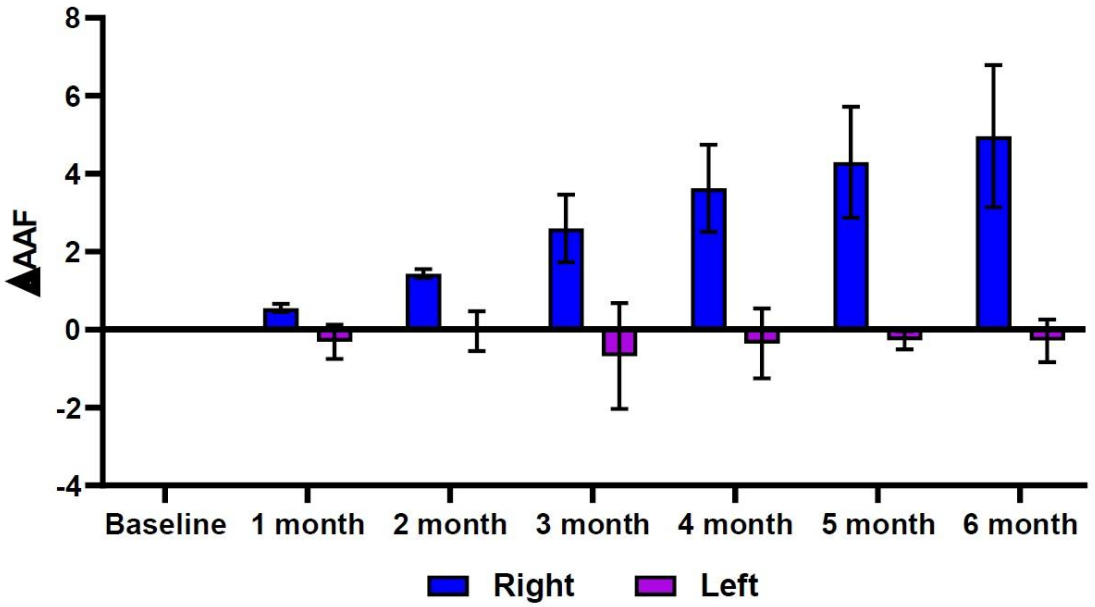

(**b**) 50 N

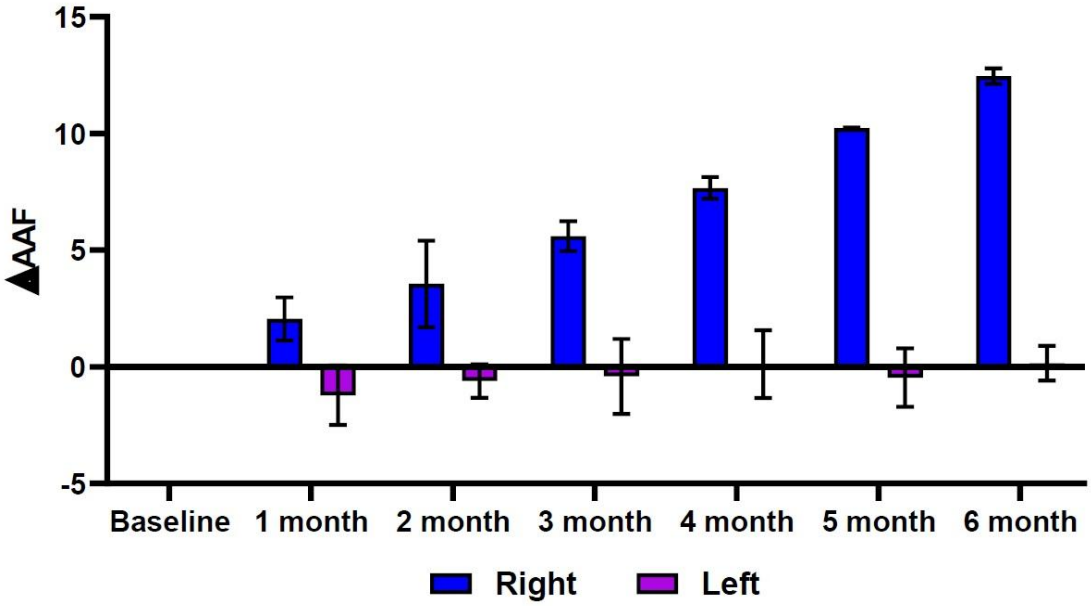

Figure 3. Changes in the anatomical axis of the femur after unilateral distraction at a force of 25 and 50 N.

 doi:10.20944/preprints202603.1757.v1

(**a**) 25 N

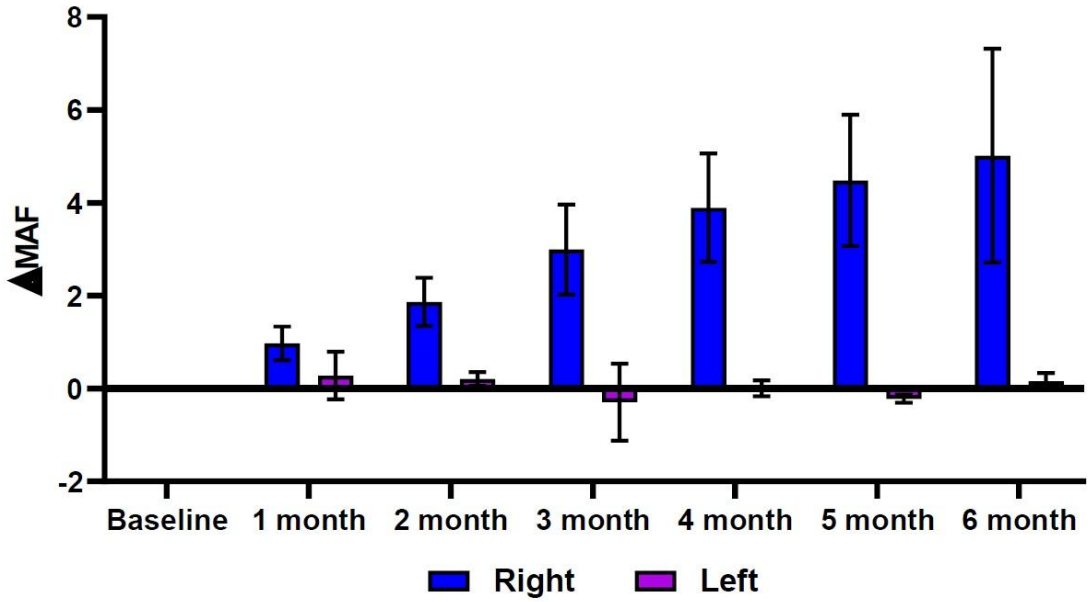

(**b**) 50 N

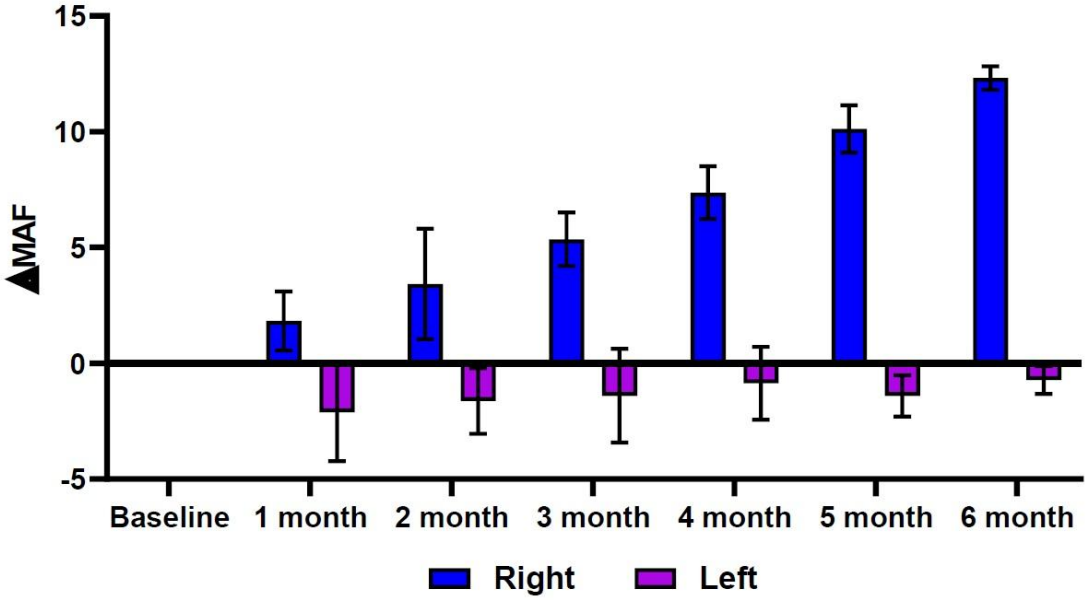

Figure 4. Changes in the mechanical axis of the femur after unilateral distraction at a force of 25 and 50 N.

4. Discussion

Bone is a dynamic anatomical structure that is involved in complex physiological phenomena characterized by an interplay between diverse cells and tissues [20]. The GP is located at the end of the ilium, and it is composed of cartilage, bone and fibrous components and then mainly involved in the longitudinal growth of the bone [21]. Thus, it finally serves as the target organ in the longitudinal growth of the bone, which is characterized by cellular level changes encompassing the proliferation and differentiation of the cartilage [22]. In association with this, according to Jaramillo D and Hoffer FA, the cartilaginous structure at the end of the bone is involved in biological mechanisms underlying the bone growth [23]. Moreover, Frost HM reported that a better understanding of the physiology of GP would be applicable to other specialty areas. More specifically, this author reported that it would be mandatory to differentiate between the bone with a higher level of mechanical activity and that with a lower level of mechanical activity, to increase and then maintain the strength of growing bone

 doi:10.20944/preprints202603.1757.v1

and to assess the strength and health of the bone based on its physiological responses [24]. In particular, both growth factors and mechanical loads are essential factors of the development and growth of cartilage. This deserves special attention from perspectives of clinicians [25].

The longitudinal growth of the bone is mainly controlled by the alteration in the GP [26]. To date, most of the studies about the GP have been conducted in an experimental setting using animals, such as rats or rabbits. These studies have shown that the cell division, the proliferation of the GP cartilage and the synthesis and degradation of extracellular matrix [27–29]. Moreover, it has also been shown that the height of the GP has a relationship with the growth rate of rats [30]. Nevertheless, there is a paucity of previous literatures regarding the factors involved in the morphological changes in the GP and their association with somatic growth in humans. Craig JG, et al. analyzed age-related changes in the size of the GP in a pediatric population, thus reporting that there is an approximately linear relationship between the surface area of the GP and the age [31].

The GP is located at the end of the femur and tibia in the lower extremities; the length of these two long bones is a critical factor of the longitudinal growth [12,32–35]. Based on these previous published studies, we strived to develop a new concept of non-osteotomy implant that promotes the bone growth by distracting the GP.

Advantages of a new concept of non-osteotomy implant, described herein, include the promotion of the bone growth with no damages to the GP, resulting in the safety of the surgical procedure, and the placement of the first bar on the medial side of the GP for the penetration into the metaphysis and that of the second bar on the lateral side of the GP for the penetration into the epiphysis. This should ensure *not only* that both the first and second bars should be placed in the adjacent region to the external surface of the target long bone and in the skin tissue surrounding it *but also* that the GP should be distracted through the maximization of the gap between the two bars.

To summarize, our results are as follows:

(1) The mean maximum load was measured as 754.33±66.88 N. These results suggest that a new concept of non-osteotomy implant might cause no damages to the GP.

(2) There were no notable clinical findings and death of experimental animals in association with study treatments during the experimet. In the polar negative control, the weight of the experimental animal at days 0 and 24 was measured as 323.72±20.84 g and 446.94±26.45 g, respectively. In the negative control, these measurements were 319.84±17.32 g and 460.30±27.05 g in the corresponding order. Moreover, following a comparison of the weight between after 3 days and study treatments, there were no experimental animals showing a more than 10% decrease in the weight. Furthermore, there were no notable autopsy findings whose occurrence might have a causal relationship with study treatments.

(3) With bilateral distraction at a tensile force of 50 N and 100 N, the degree of changes in the length of the AAF at 1 month from baseline was higher on the right side as compared with the left side. This was also seen in the length of the MAF. Moreover, with unilateral distraction at a tensile force of 25 N and 50 N, the degree of changes in the angle formed by the AAF at 1, 2, 3, 4, 5 and 6 months from baseline was significantly higher on the right side as compared with the left side ($P<0.05$). This was also seen in the angle formed by the MAF.

But our results cannot be generalized because the current experiment used a small number of animals. A greater number of experimental animals should therefore be used for further studies.

5. Conclusions

The current experimental results confirm the biological safety, the biocompatibility and biomechanical effectiveness of a new-concept of non-osteotomy implant in promoting the bone growth. But this deserves further prospective randomized controlled trials.

Author Contributions: Conceptualization, T.R.; data curation, T.R.; formal analysis, T.R.; investigation, T.R.; methodology, T.R.; supervision, T.R.; writing—original draft, T.R.; writing—review and editing, T.R.

Institutional Review Board Statement: Non-applicable.

 doi:10.20944/preprints202603.1757.v1

Acknowledgments: The author thanks Laon Medi Solution Inc. (Seoul, Republic of Korea) and KDH Medical Inc. (Gwangmyeong, Gyeonggi, Republic of Korea) for additional support of this study.

Conflicts of Interest: The author has nothing to declare in relation to this work.

References

1. Blakemore, S.J.; Burnett, S.; Dahl, R.E. The role of puberty in the developing adolescent brain. *Hum. Brain Mapp.* **2010,** *31,* 926–933.
2. Güngör, N.K. Overweight and obesity in children and adolescents. *J. Clin. Res. Pediatr. Endocrinol.* **2014,** *6,* 129–143.
3. Lin, X.; Aris, I.M.; Tint, M.T.; Soh, S.E.; Godfrey, K.M.; Yeo, G.S.; Kwek, K.; Chan, J.K.; Gluckman, P.D.; Chong, Y.S.; Yap, F.; Holbrook, J.D.; Lee, Y.S. Ethnic differences in effects of maternal pre-pregnancy and pregnancy adiposity on offspring size and adiposity. *J. Clin. Endocrinol. Metab.* **2015,** *100,* 3641–3650.
4. Natale, V.; Rajagopalan, A. Worldwide variation in human growth and the World Health Organization growth standards: A systematic review. *BMJ Open* **2014,** *4,* e003735.
5. Emons, J.; Chagin, A.S.; Sävendahl, L.; Karperien, M.; Wit, J.M. Mechanisms of growth plate maturation and epiphyseal fusion. *Horm. Res. Paediatr.* **2011,** *75,* 383–391.
6. Haraguchi, R.; Kitazawa, R.; Kohara, Y.; Ikedo, A.; Imai, Y.; Kitazawa, S. Recent insights into long bone development: Central role of Hedgehog signaling pathway in regulating growth plate. *Int. J. Mol. Sci.* **2019,** *20,* 5840.
7. Ağırdil, Y. The growth plate: A physiologic overview. *EFORT Open Rev.* **2020,** *5,* 498–507.
8. Gubin, A.V.; Borzunov, D.Y.; Malkova, T.A. The Ilizarov paradigm: Thirty years with the Ilizarov method, current concerns and future research. *Int. Orthop.* **2013,** *37,* 1533–1539.
9. Baloch, S.R.; Rafi, M.S.; Junaid, J.; Shah, M.; Siddiq, F.; Ata-Ur-Rahman, S.; Zohaib, Z. Ilizarov fixation method of tibial plateau fractures: A prospective observational study. *Cureus* **2020,** *12,* e11277.
10. Pornrattanamaneewong, C.; Numkanisorn, S.; Chareancholvanich, K.; Harnroongroj, T. A retrospective analysis of medial opening wedge high tibial osteotomy for varus osteoarthritic knee. *Indian J. Orthop.* **2012,** *46,* 455–461.
11. Saran, N.; Rathjen, K.E. Guided growth for the correction of pediatric lower limb angular deformity. *J. Am. Acad. Orthop. Surg.* **2010,** *18,* 528–536.
12. Hasler, C.C.; Krieg, A.H. Current concepts of leg lengthening. *J. Child Orthop.* **2012,** *6,* 89–104.
13. Fragomen, A.T.; Rozbruch, S.R. The mechanics of external fixation. *HSS J.* **2007,** *3,* 13–29.
14. Alqahtani, M.S.; Al-Tamimi, A.A.; Hassan, M.H.; Liu, F.; Bartolo, P. Optimization of a patient-specific external fixation device for lower limb injuries. *Polymers* **2021,** *13,* 2661.
15. Bråten, M.; Helland, P.; Grøntvedt, T.; Aamodt, A.; Benum, P.; Mølster, A. External fixation versus locked intramedullary nailing in tibial shaft fractures: A prospective, randomized study. *Arch. Orthop. Trauma Surg.* **2005,** *125,* 21–26.
16. Mshana, R.N.; Tadesse, G.; Abate, G.; Miörner, H. Use of 3-(4,5-dimethylthiazol-2-yl)-2,5-diphenyl tetrazolium bromide for rapid detection of rifampin-resistant Mycobacterium tuberculosis. *J. Clin. Microbiol.* **1998,** *36,* 1214–1219.
17. Kimber, I.; Basketter, D.A.; Berthold, K.; Butler, M.; Garrigue, J.L.; Lea, L.; Newsome, C.; Roggeband, R.; Steiling, W.; Stropp, G.; Waterman, S.; Wiemann, C. Skin sensitization testing in potency and risk assessment. *Toxicol. Sci.* **2001,** *59,* 198–208.
18. Mohamed Thajudeen, M.Z.; Mahmood Merican, A.; Hashim, M.S.; Nordin, A. The utility of lesser trochanter version to estimate femoral anteversion in total hip arthroplasty: A three-dimensional computed tomography study. *Surg. Tech. Dev.* **2022,** *11,* 54–61.
19. Cyteval, C. Imaging of knee implants and related complications. *Diagn. Interv. Imaging* **2016,** *97,* 809–821.
20. Odgren, P.R.; Philbrick, W.M.; Gartland, A. Osteoclastogenesis and growth plate chondrocyte differentiation: Emergence of convergence. *Crit. Rev. Eukaryot. Gene Expr.* **2003,** *13,* 181–193.
21. Iannotti, J.P. Growth plate physiology and pathology. *Orthop. Clin. North Am.* **1990,** *21,* 1–17.

 doi:10.20944/preprints202603.1757.v1

22. van der Eerden, B.C.; Karperien, M.; Wit, J.M. Systemic and local regulation of the growth plate. *Endocr. Rev.* **2003,** *24,* 782–801.
23. Jaramillo, D.; Hoffer, F.A. Cartilaginous epiphysis and growth plate: Normal and abnormal MR imaging findings. *AJR Am. J. Roentgenol.* **1992,** *158,* 1105–1110.
24. Frost, H.M. From Wolff's law to the Utah paradigm: Insights about bone physiology and its clinical applications. *Anat. Rec.* **2001,** *262,* 398–419.
25. Darling, E.M.; Athanasiou, K.A. Biomechanical strategies for articular cartilage regeneration. *Ann. Biomed. Eng.* **2003,** *31,* 1114–1124.
26. Villemure, I.; Stokes, I.A. Growth plate mechanics and mechanobiology: A survey of present understanding. *J. Biomech.* **2009,** *42,* 1793–1803.
27. Kember, N.F. Comparative patterns of cell division in epiphyseal cartilage plates in the rabbit. *J. Anat.* **1985,** *142,* 185–190.
28. Hunziker, E.B.; Schenk, R.K. Physiological mechanisms adopted by chondrocytes in regulating longitudinal bone growth in rats. *J. Physiol.* **1989,** *414,* 55–71.
29. Ballock, R.T.; O'Keefe, R.J. The biology of the growth plate. *J. Bone Joint Surg. Am.* **2003,** *85,* 715–726.
30. Wilsman, N.J.; Farnum, C.E.; Green, E.M.; Lieferman, E.M.; Clayton, M.K. Cell cycle analysis of proliferative zone chondrocytes in growth plates elongating at different rates. *J. Orthop. Res.* **1996,** *14,* 562–572.
31. Craig, J.G.; Cody, D.D.; Van Holsbeeck, M. The distal femoral and proximal tibial growth plates: MR imaging, three-dimensional modeling and estimation of area and volume. *Skeletal Radiol.* **2004,** *33,* 337–344.
32. Lui, J.C.; Jee, Y.H.; Garrison, P.; Iben, J.R.; Yue, S.; Ad, M.; Nguyen, Q.; Kikani, B.; Wakabayashi, Y.; Baron, J. Differential aging of growth plate cartilage underlies differences in bone length and skeletal proportions. *PLoS Biol.* **2018,** *16,* e2005263.
33. Pines, M.; Hurwitz, S. The role of the growth plate in longitudinal bone growth. Poult. Sci. 1991, 70, 1806–1814.
34. Pritchett, J.W. Longitudinal growth and growth-plate activity in the lower extremity. *Clin. Orthop. Relat. Res.* **1992,** *275,* 274–279.
35. Wang, X.; Li, Z.; Wang, C.; Bai, H.; Wang, Z.; Liu, Y.; Bao, Y.; Ren, M.; Liu, H.; Wang, J. Enlightenment of growth plate regeneration based on cartilage repair theory: A review. *Front. Bioeng. Biotechnol.* **2021,** *9,* 654087.